

CONVECTIVE HEAT TRANSFER IN MICROSCALE SLIP FLOW

A. GUVENC YAZICIOGLU¹ AND S. KAKAÇ²

¹*Orta Doğu Teknik Üniversitesi, Makine Mühendisliği Bölümü,
Ankara, 06531 Turkey, agyazi@gmail.com*

²*TOBB Ekonomi ve Teknoloji Üniversitesi, Makine Mühendisliği
Bölümü, Söğütözü Cad.No:43, Söğütözü, Ankara, 06560 Turkey*

Abstract. In this lecture, steady-state convective heat transfer in different microchannels (microtube and parallel plates) will be presented in the slip flow regime. Laminar, thermally and/or hydrodynamically developing flows will be considered. In the analyses, in addition to rarefaction, axial conduction, and viscous dissipation effects, which are generally neglected in macroscale problems, surface roughness effects, and temperature-variable thermophysical properties of the fluid will also be taken into consideration. Navier–Stokes and energy equations will be solved and the variation of Nusselt number, the dimensionless parameter for convection heat transfer, along the channels will be presented in tabular and graphical forms as a function of Knudsen, Peclet, and Brinkman numbers, which represent the effects of rarefaction, axial conduction, and viscous dissipation, respectively. The results will be compared and verified with available experimental, analytical, and numerical solutions in literature.

1. Introduction

Devices having the dimensions of microns have been used in many fields such as; biomedicine, diagnostics, chemistry, electronics, automotive industry, space industry, and fuel cells, to name a few. With the increase of integrated circuit density and power dissipation of electronic devices, it is becoming more necessary to employ effective cooling devices and cooling methods to maintain the operating temperature of electronic components at a safe level. Especially when device dimensions get smaller, overheating of micro-electronic components may be a serious issue. Microchannel heat sinks, with hydraulic diameters ranging from 10 to 1,000 μm , appear to be the ultimate solution for removing these high amounts of heat. This pressing requirement of cooling of electronic devices has initiated extensive research in microchannel heat transfer. Many analytical and experimental studies have been performed to have a better understanding of heat transfer at the

microscale. Both liquids and gases have been investigated. However, none of them has been able to come to a general conclusion. For example, there are controversial results in the literature about the boundary conditions, for liquids flows. It is not clear whether discontinuity of velocity and temperature exists on the wall or not.

The pioneering conclusion drawn by Tuckerman and Pease in 1982 [1] that the heat transfer coefficient for laminar flow through microchannels may be greater than that for turbulent flow, accelerated research in this area. Many experimental [2–6], numerical [7–10], and analytical [11–14] studies have been performed, with some focusing on the effects of roughness [15–21] and temperature-variable thermophysical properties of the fluid [22–26].

Some of these works have been compiled in review articles such as those by Gad-El-Hak [27], Morini [28], Bayazitoglu [29], Hetsroni [30], Yener [31], Cotta [32], and Rosa [33]. The reader is also referred to excellent books by Karniadakis [34], Sobhan [35], and Yarin [36].

Several conflicting results may be drawn from the above-mentioned studies. First, some investigators reported laminar fully-developed friction factors and Poiseuille numbers lower than the conventional values, some reported higher values, while others reported agreement with conventional values. Another conflict occurs in laminar to turbulent transition Re values, varying between 3,000 and 6,000. A similar conclusion can be made about the laminar regime Nusselt number ($Nu = hD/k$, h being the convection heat transfer coefficient, and D the hydraulic diameter) and the effect of energy dissipation on heat transfer. However, it should also be noted that as the precision and reliability of the experimental set-ups and measurement devices increase, the deviation margin of theoretical and experimental results obtained from similar experiments conducted by different investigators reduces. In any case, future research is still needed for fundamental understanding, as pointed out in Refs. [28–33, 37, 38].

2. General Considerations

For the effective and economical design of microchannel heat sinks, some key design parameters should be considered and optimized. These are, the pressure required for pumping the cooling fluid, the mass flow rate of the cooling fluid, the hydraulic diameter of the channels, the temperature of the fluid and the channel wall, and the number of channels. In order to understand the effect of these parameters on the system, the dynamic behavior and heat transfer characteristics of fluids at the microscale must be well-understood.

There are two major approaches to modeling fluid flow at the microscale: In the first model, the molecular model, the fluid is assumed to be a collection of molecules whereas in the second model, the continuum model, the fluid

is assumed to be continuous and indefinitely divisible. In macroscale flows, the continuum approach is generally accepted. The velocity, density, pressure, etc., for the fluid are defined at every point and time in space. Conservation of mass, momentum, and energy are applied and a set of nonlinear partial differential equations (Navier–Stokes and energy equations) are obtained. These equations are solved to obtain the fluid flow and heat transfer characteristic parameters at the macroscale. However as the dimensions of the channels get smaller, the continuum assumption starts to break. For microscale slip flow regime, the continuum approach is still valid, and Navier–Stokes and energy equations may still be used, but with a modification of boundary conditions.

One important dimensionless parameter characterizing the flow regime is the Knudsen number (Kn). Knudsen number, which signifies the degree of rarefaction in the flow and the degree of validity of the continuum model, is defined as the ratio of the mean free path of the molecules, λ , to the characteristic length, L ($\text{Kn} = \lambda/L$). The different Kn regimes are determined empirically and are therefore only approximate for a particular flow geometry. For example, for gases, below $L \approx 100$ nm, the rarefaction effect seems to be significant, while for liquids, below $L \approx 0.3$ nm, the interfacial electro-kinetic effects near the solid–liquid interface become important. In general, the following is a commonly used scale for Kn to differentiate flow regimes [34]:

$\text{Kn} < 0.001$	Continuum flow
$0.001 < \text{Kn} < 0.1$	Slip-flow (slightly rarefied)
$0.1 < \text{Kn} < 10$	Transition flow (moderately rarefied)
$\text{Kn} > 10$	Free-molecular flow (highly rarefied)

When the flow is in the higher Kn regime (transition and free-molecular), a molecular approach, such as direct simulation Monte Carlo method using the Boltzmann equation should be employed. For $L \gg \lambda$, the continuum approach will be applicable with traditional no-slip, no-temperature jump boundary conditions. However as this condition is violated, the linear relation between stress and the rate of strain, thus the no-slip velocity condition will not be valid. Similarly, the linear relation between heat flux and temperature gradient, thus the no-temperature jump condition at the solid–fluid interface will no longer be accurate [39]. The fluid and solid particles cannot retain thermodynamic equilibrium at the surface, thus the fluid molecules close to the surface do not have the velocity and temperature of the surface. Therefore, the slip-flow regime may be modeled with classical Navier–Stokes and energy equations by making some modifications in the boundary conditions for velocity and temperature at the wall, because the rarefaction effect is not small enough to be negligible in the slip-flow regime. As a result, fluid molecules at the wall will have finite slip-velocity and temperature-jump at

the wall. These modified conditions depend on the Kn value, some thermophysical properties of the fluid, and accommodation factors.

Besides the Knudsen number, some other dimensionless parameters become important in microscale flow and heat transfer problems. The first such number is the Peclet number (Pe), which is the product of Reynolds (Re) and Prandtl (Pr) numbers ($Pe = Re \cdot Pr$), and signifies the ratio of rates of advection to diffusion. Peclet number enumerates the axial conduction effect in flow. In macro-sized conduits, Pe is generally large and the effect of axial conduction may be neglected. However as the channel dimensions get smaller, it may become important.

Brinkman number is the dimensionless parameter representing the relative importance of heat generated by viscous dissipation (work done against viscous shear) to heat transferred by fluid conduction across the microchannel cross-section in the flow. Its definition varies with the boundary condition at the wall. For example, for constant wall temperature, $Br = \mu u_m^2 / k \Delta T$ and for constant wall heat flux, $Br = \mu u_m^2 / q_w R$, where μ is the fluid dynamic viscosity, u_m is the mean flow velocity, k is the fluid thermal conductivity, ΔT is the fluid inlet-to-wall temperature difference, R is the hydraulic radius of the channel, and q_w is the wall heat flux. Br is usually neglected in low-speed and low-viscosity flows through conventionally-sized channels of short lengths. However in flows through conventionally-sized long pipelines, Br may become important. For flows in microchannels, the length-to-diameter ratio can be as large as for flows through conventionally-sized long pipelines, thus Br may become important in microchannels as well.

In this lecture, the effects of the abovementioned dimensionless parameters, namely, Knudsen, Peclet, and Brinkman numbers representing rarefaction, axial conduction, and viscous dissipation, respectively, will be analyzed on forced convection heat transfer in microchannel gaseous slip flow under constant wall temperature and constant wall heat flux boundary conditions. Nusselt number will be used as the dimensionless convection heat transfer coefficient. A majority of the results will be presented as the variation of Nusselt number along the channel for various Kn, Pe, and Br values. The lecture is divided into three major sections for convective heat transfer in microscale slip flow. First, the principal results for microtubes will be presented. Then, the effect of roughness on the microchannel wall on heat transfer will be explained. Finally, the variation of the thermophysical properties of the fluid will be considered.

3. Microtubes

The geometry of the problem for microtubes is shown in Fig. 1. Steady-state, two-dimensional, incompressible, laminar, and single-phase gas flow is considered. An unheated section is provided, where the velocity profile

develops. As mentioned before, in the slip flow regime, slip-velocity and temperature-jump boundary conditions should be applied to the momentum and energy equations. These are:

$$u_s = -\frac{2-F_m}{F_m} \lambda \left(\frac{du}{dr} \right)_{r=R} \quad (1)$$

$$T_s - T_w = -\frac{2-F_t}{F_t} \frac{2\gamma}{\gamma+1} \frac{\lambda}{Pr} \left(\frac{\partial T}{\partial r} \right)_{r=R} \quad (2)$$

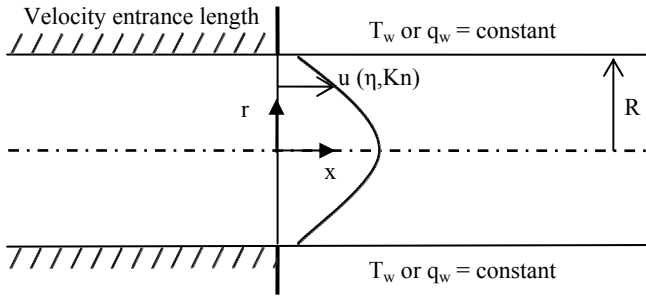


Figure 1. The problem geometry for microtubes.

In Eq. (1), F_m is the momentum accommodation factor and has a value close to unity for the gas–solid couples used most commonly in engineering, and is also taken so in this work. In Eq. (2), T_s is the temperature of the fluid molecules at the wall, T_w is the wall temperature, γ is the ratio of the specific heats of the fluid, and F_t is the thermal accommodation factor. F_t may take a value in the range 0.0–1.0, depending on the gas and solid surface, the gas temperature and pressure, the temperature difference between the gas and the surface, and is determined experimentally.

Using the slip-velocity boundary condition, the fully developed velocity profile may be written as [40]

$$\frac{u}{u_m} = \frac{2(1-\eta^2) + 8Kn}{1 + 8Kn}, \quad (3)$$

where $\eta = r/R$ is the nondimensional radial coordinate. Figure 2 presents the variation of the nondimensional velocity along the radial distance as a function of rarefaction in the flow. As can be observed therein, for continuum ($Kn = 0$), the no-slip velocity is present at the wall while as the degree of rarefaction increases, so does the slip velocity at the wall [41].

3.1. CONSTANT WALL TEMPERATURE

For this boundary condition, the nondimensional energy equation and the boundary conditions for the flow inside a microtube, including axial conduction and viscous dissipation are

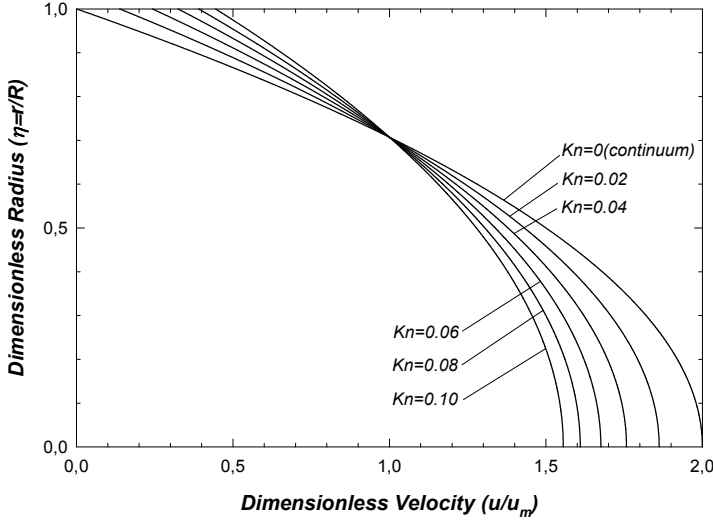


Figure 2. Velocity profile variation with Kn along the radial direction.

$$\frac{u^*}{2} \frac{\partial \theta}{\partial \xi} = \frac{1}{\eta} \frac{\partial}{\partial \eta} \left(\eta \frac{\partial \theta}{\partial \eta} \right) + \frac{1}{\text{Pe}^2} \frac{\partial^2 \theta}{\partial \xi^2} + \text{Br} \left(\frac{\partial u^*}{\partial \eta} \right)^2, \quad (4)$$

$$\eta = 0, \quad \frac{\partial \theta}{\partial \eta} = 0, \quad (5)$$

$$\eta = 1, \quad \theta = -2\kappa \text{Kn} \left(\frac{\partial \theta}{\partial \eta} \right)_{\eta=1}, \quad (6)$$

$$\xi = 0, \quad \theta = 1. \quad (7)$$

In Eqs. (4–7), the following parameters have been used for non-dimensionalization:

$$\theta = \frac{T - T_w}{T_i - T_w}, \quad \text{Br} = \frac{\mu u_m^2}{k(T_i - T_w)}, \quad \xi = \frac{x}{\text{Pe}R}, \quad \eta = \frac{r}{R}, \quad u^* = \frac{u}{u_m}, \quad (8)$$

and κ is a parameter that accounts for temperature jump at the wall as

$$\kappa = \frac{2 - F_t}{F_t} \frac{2\gamma}{\gamma + 1} \frac{1}{Pr}. \quad (9)$$

The energy equation has been solved numerically [40] and analytically, using general Eigen functions expansion [42], and the details can be found in related references. Using the temperature distribution, the local Nusselt number may be determined as

$$Nu_x = \frac{h_x D}{k} = - \frac{2 \frac{\partial \theta}{\partial \eta} \Big|_{\eta=1}}{\theta_m - \frac{4\gamma}{\gamma + 1} \frac{Kn}{Pr} \frac{\partial \theta}{\partial \eta} \Big|_{\eta=1}}, \quad (10)$$

where θ_m is the nondimensional mean temperature defined by

$$\theta_m(\xi) = 2 \int_0^1 u^* \theta(\eta, \xi) \eta d\eta. \quad (11)$$

3.2. CONSTANT WALL HEAT FLUX

In this case, the nondimensional energy equation and the boundary conditions become [40],

$$\frac{Gz(1 - \eta^2 + 4Kn)}{2(1 + 8Kn)} \frac{\partial \theta}{\partial \zeta} = \frac{1}{\eta} \frac{\partial}{\partial \eta} \left(\eta \frac{\partial \theta}{\partial \eta} \right) + \frac{1}{Pe^2} \frac{\partial^2 \theta}{\partial \zeta^2} + \frac{32Br}{(1 + 8Kn)^2} \eta^2, \quad (12)$$

$$\eta = 0, \quad \frac{\partial \theta}{\partial \eta} = 0, \quad (13)$$

$$\eta = 1, \quad \frac{\partial \theta}{\partial \eta} = 1, \quad (14)$$

$$\xi = 0, \quad \theta = 1. \quad (15)$$

In Eqs. (12–15) the following additional parameters have been used for non-dimensionalization:

$$\theta = \frac{k(T - T_i)}{q_w R}, \quad Br = \frac{\mu u_m^2}{q_w D}, \quad Gz = \frac{2R}{L} Re Pr, \quad (16)$$

The temperature profile is determined numerically, and using the temperature distribution, local Nusselt number may be determined as [40],

$$Nu_x = \frac{h_x D}{k} = - \frac{2}{\theta_s + \frac{4\gamma}{\gamma + 1} \frac{Kn}{Pr} - \theta_m}, \quad (17)$$

where θ_s is the nondimensional temperature of the fluid at the surface.

3.3. RESULTS

In this section, the results will be presented in tabular and graphical forms, for Nusselt number for both constant wall temperature and constant wall heat flux cases with variable Kn, Br, Pe values to investigate the effects of rarefaction, viscous dissipation, and axial conduction in the slip-flow regime for microtubes. Table 1 presents the effect of rarefaction on laminar flow fully developed Nu values for constant wall temperature (Nu_T) and constant wall heat flux (Nu_q) cases, where viscous dissipation and axial

TABLE 1. Laminar flow fully-developed Nu values for the present work for constant wall temperature (Nu_T) and constant wall heat flux (Nu_q) cases, compared with analytical results from Ref. [43] ($Pr = 0.6$).

Kn	Nu_T [43]	Nu_T	Nu_q [43]	Nu_q
0.00	3.6751	3.6566	4.3627	4.3649
0.02	3.3675	3.3527	3.9801	4.0205
0.04	3.0745	3.0627	3.5984	3.6548
0.06	2.8101	2.8006	3.2519	3.3126
0.08	2.5767	2.5689	2.9487	3.0081
0.10	2.3723	2.3659	2.6868	2.7425

conduction effects have been neglected. The table serves as a verification of the solution procedure, as comparisons with analytical solutions from literature [43] are also provided.

To observe the effect of viscous dissipation on heat transfer, in Table 2, the fully developed Nusselt number is presented for constant wall temperature and constant wall heat flux cases with and without viscous dissipation. For all cases, the fully developed Nusselt number decreases as Kn increases. For $T_w = \text{constant}$, for the no-slip condition ($Kn = 0$), when $Br = 0.01$, $Nu = 9.5985$, while it drops down to 3.8227 for $Kn = 0.1$, a decrease of 60.2%. Similarly for $q_w = \text{constant}$, for the no-slip condition, when $Br = 0.01$, $Nu = 4.1825$, while it drops down to 2.9450 for $Kn = 0.1$, with a decrease of 29.6%. This is due to the fact that the temperature jump, which increases with increasing rarefaction, reduces heat transfer, as can be observed from Eqs. (10) and (17). A negative Br value for the constant wall heat flux condition refers to the fluid being cooled, therefore Nu takes higher values for $Br < 0$ and lower values for $Br > 0$ compared with those for no viscous heating.

TABLE 2. Laminar flow fully-developed Nu with and without viscous dissipation for $T_w = \text{constant}$ and $q_w = \text{constant}$ cases ($Pr = 0.7$).

Kn	$T_w = \text{constant}$		$q_w = \text{constant}$		
	$Br = 0.00$	$Br = 0.01$	$Br = 0.00$	$Br = 0.01$	$Br = -0.01$
0.00	3.6566	9.5985	4.3649	4.1825	4.5640
0.02	3.4163	7.4270	4.1088	4.0022	4.2212
0.04	3.1706	6.0313	3.8036	3.7398	3.8695
0.06	2.9377	5.0651	3.4992	3.4598	3.5395
0.08	2.7244	4.3594	3.2163	3.1912	3.2419
0.10	2.5323	3.8227	2.9616	2.9450	2.9784

In Fig. 3, the variation of local Nusselt number along the constant wall temperature tube is presented as a function of Peclet number, representing axial conduction in the fluid. For $Pe = 50$, which represents a case with negligible axial conduction, the solution of the classical Graetz problem, $Nu = 3.66$, is reached [44], while for $Pe = 1$, $Nu = 4.03$ [45] is obtained as the fully developed values of Nu . The temperature gradient at the wall decreases at low Pe values, thus the local and fully developed Nu values increase with decreasing Pe .

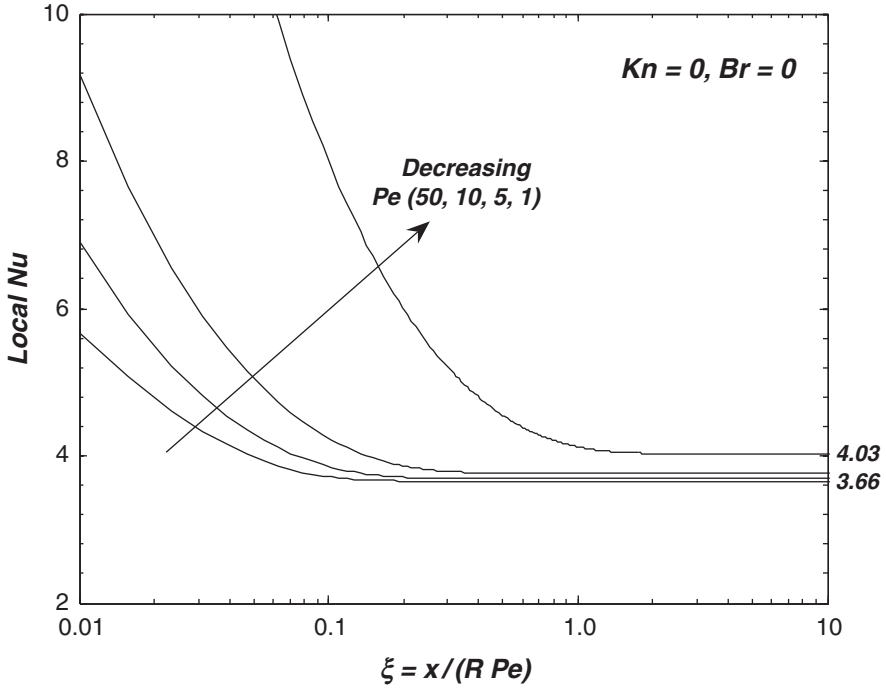


Figure 3. Variation of local Nu with Pe when $Kn = 0$ and $Br = 0$.

Figure 4 presents the local Nusselt number variation along the microtube for the constant wall temperature boundary condition for cases where both viscous dissipation and axial conduction effects have been considered. A positive Br for this boundary condition refers to the fluid being cooled as it flows along the tube. Local Nu value first decreases due to temperature jump at the wall, then increases to its fully-developed value because of the heating due to the viscous dissipation effect. Before the increase, the values of local Nu match those for the $Br = 0$ case presented in Fig. 3 [10, 42]. However, because of the definition of Pe , local Nu curves deviate from those for $Br = 0$ as the minima are approached. This effect results in the overall increase in the average Nu in the tube, thus we can conclude that average Nu increases as the effect of axial conduction is more prominent. Also, the amount of viscous dissipation does not affect the fully developed Nu value.

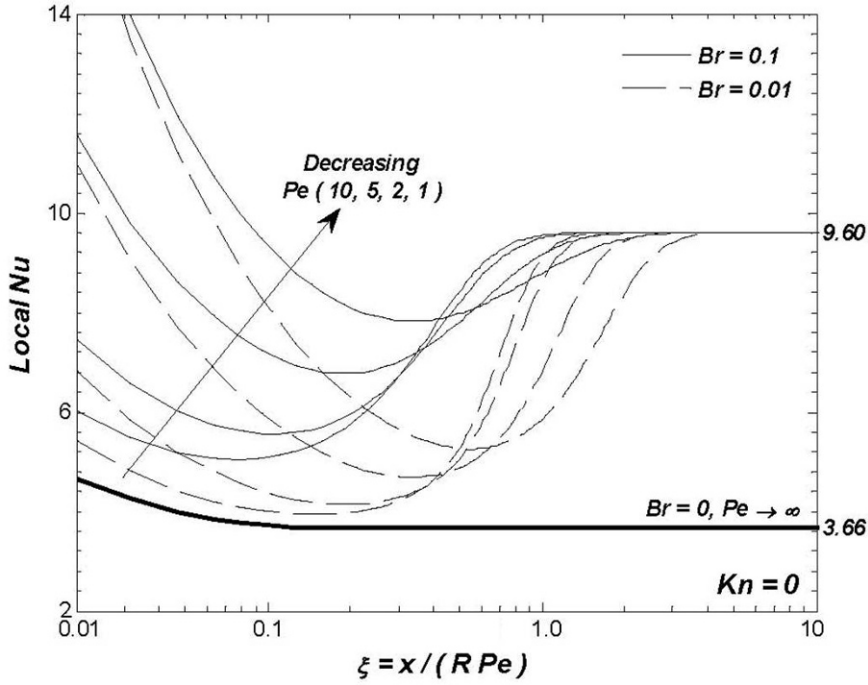


Figure 4. Variation of local Nu with Pe when viscous dissipation is present ($Br > 0$, $Kn = 0$).

When the fluid is being heated along the tube, i.e., the fluid inlet temperature is less than that of the wall, for the constant wall temperature case, Br is negative and the local Nu variation is as shown in Fig. 5. As can be observed therein, local Nu reaches an asymptotic value when the fluid temperature is equal to the wall temperature, when viscous dissipation and axial conduction are included. Thermal development continues after this point, and the fully developed Nu is reached. Similar to positive Br cases, the amount of viscous dissipation effects the location where the sudden change in local Nu occurs, but the fully developed Nu is the same for all non-zero Br values.

Table 3 summarizes a majority of the results for fully developed Nu for slip-flow in microtubes presented in this section for constant wall temperature boundary condition, and provides comparisons with available results from literature. Here, $\kappa = 0$ refers to no temperature jump while $\kappa = 1.667$ refers to temperature jump for air flow. The present results show excellent agreement with literature.

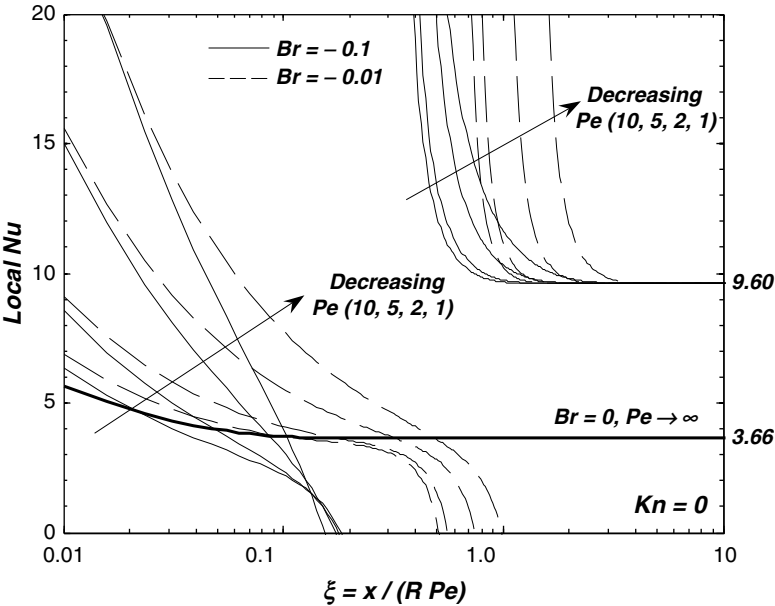


Figure 5. Variation of local Nu with Pe when viscous dissipation is present ($Br < 0$, $Kn = 0$).

TABLE 3. Comparison of fully developed Nu with results from literature.

Kappa (κ)	Pe = 1.0		Pe = 5.0		Pe = 10		Pe $\rightarrow \infty$		Kn
	Nu	Nu*	Nu	Nu**	Nu	Nu*	Nu	Nu***	
0	4.028	4.030	3.767	3.767	3.695	3.697	3.656	3.656	0.00
1.667	4.028	4.030	3.767	3.767	3.695	3.697	3.656	3.656	
0	4.358	—	4.131	—	4.061	—	4.020	4.020	0.04
1.667	3.604	—	3.387	—	3.325	—	3.292	3.292	
0	4.585	—	4.386	—	4.319	—	4.279	4.279	0.08
1.667	3.093	—	2.949	—	2.909	—	2.887	2.887	

Nu: Present results

Nu* : Results from Ref. [45]

Nu** : Results from Ref. [46]

Nu*** : Results from Ref. [9]

4. Roughness Effect

The effect of surface roughness may be particularly important in microchannel flows. Roughness characteristics of microchannels are strictly dependent on the manufacturing process. Since the random distribution and small size of the roughness peaks along a surface are quite difficult to define, most investigators neglect this effect in their studies. There is a limited number of publications in open literature compared to other effects in microscale. In one of the first experimental studies in this area water flow through rough

fused silica and stainless steel microtubes was investigated, and deviations from theoretical predictions; such as higher friction factor, and early transition from laminar to turbulent flow, were found [15]. Later, heat transfer characteristics were also investigated and due to the surface roughness effect, smaller Nu values were determined [47]. Different models were proposed to represent the effects of surface roughness; such as roughness-viscosity model [15], porous medium layer model [48], and the explicit model [17, 18]. Roughness can reduce or increase Nu depending on the distribution, spacing, and geometry of the obstructions. However one common conclusion is that roughness is more effective at low Kn values.

In this case, steady-state, laminar, developing air flow in a parallel-plate microchannel with one rough wall is considered. As shown in the channel schematic in Fig. 6, the roughness is modeled as two-dimensional equilateral triangular elements placed on the bottom wall surface. The relative surface roughness of the wall may be determined by $\varepsilon = e/D$, where e is the height of the roughness elements and D the hydraulic diameter of the channel. In most of the studies in literature, it is stated that silicon microchannels generally have a relative roughness value in the range 0–4%. Thus, in this work, $\varepsilon = 1.325\%$, 2.0% are considered [49, 50].

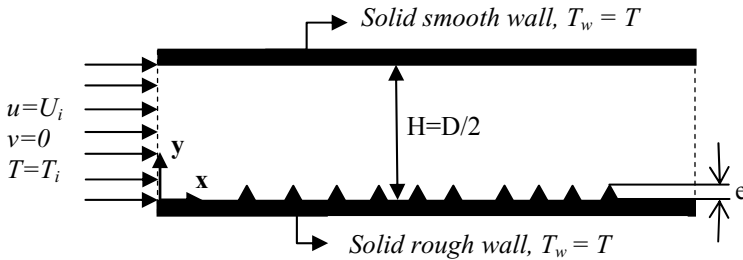


Figure 6. Schematic of the rough microchannel.

The equations to be solved are similar to those in the previous section with some minor differences due the change in geometry (parallel-plate microchannel versus microtube). In the solution, slip boundary conditions given in Eqs. (1) and (2) are applied and finite element method is used to solve for the velocity profile and the temperature distribution. Then, from the temperature profile, the local Nu is determined.

For the continuum case ($Kn = 0$), without viscous dissipation, local Nu has a wavy pattern, as shown in Fig. 7, similar to the observations in Refs. [17, 20] for triangular roughness elements. Velocity and temperature gradients are higher at the peaks of the elements, thus local Nu is larger there, while at the bottom corners, the low gradients result in minimum local Nu.

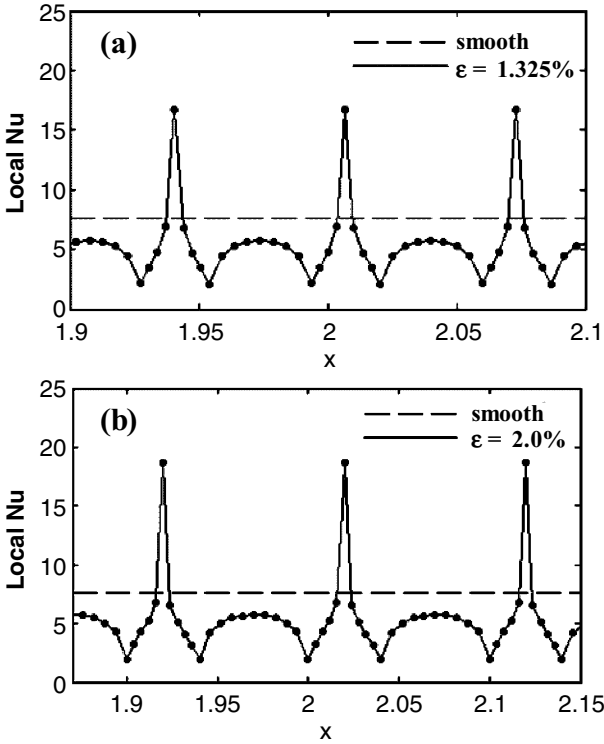


Figure 7. Local Nu variation over the roughness elements for $Kn = 0$, $Re = 100$ and $Br = 0$ when (a) $\varepsilon = 1.325\%$, (b) $\varepsilon = 2.0\%$.

Graphical results are presented in Fig. 8 for the channel averaged Nu (including smooth inlet–outlet sections), including axial conduction and viscous dissipation ($Br = 0.1$). Without the rarefaction effect, roughness reduces heat transfer. However, with the rarefaction effect, an increase in the average Nu with respect to smooth channel values is observed. Due to the reduced interaction between the gas molecules and channel walls at high Kn values, the increase is less pronounced at high Kn values and more at low Kn values. Moreover, when rarefaction is considered, the average Nu values increase with increasing Pe and relative surface roughness height. In Table 4, average Nu values for the rough section of the channel (representing a channel with a completely rough wall from the inlet to the outlet) are presented for cases where axial conduction and viscous dissipation ($Br = 0.1$) are both included, compared to smooth channel values. For this case, average Nu takes higher values, except $Kn = 0$ cases, where the reduction in local Nu between roughness elements is dominant and cannot be compensated by the higher local Nu computed at the other parts of the channel. The

general trend is similar to the channel averaged cases presented in Fig. 8; at low Kn, the effect of surface roughness is more prominent and average Nu increases with increasing roughness height. As the flow becomes more rarefied, the importance of relative surface roughness height is reduced and yields nearly the same average Nu values for the considered relative roughness heights.

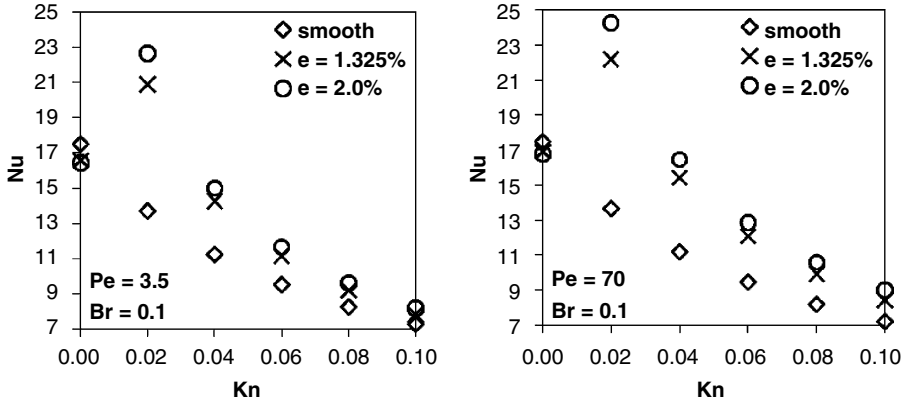


Figure 8. Channel averaged Nu compared with fully developed smooth channel values when axial conduction and viscous dissipation ($Br = 0.1$) are included.

TABLE 4. Rough section averaged Nu compared with fully developed smooth channel values when axial conduction and viscous dissipation are included ($Br = 0.1$).

Pe	Kn	Smooth	Rough 1.325%	Rough 2.0%
3.5	0.00	17.484	11.389	11.175
	0.02	13.680	26.499	29.783
	0.04	16.450	17.768	16.450
	0.06	12.289	13.160	12.289
	0.08	9.782	10.466	9.782
	0.10	8.090	8.662	8.090
70	0.00	17.547	11.585	11.384
	0.02	13.775	28.354	32.332
	0.04	11.298	18.330	20.324
	0.06	9.563	13.820	15.345
	0.08	8.280	11.062	12.340
	0.10	7.295	9.184	10.295

5. Temperature-Variable Thermophysical Properties

The earliest studies related to thermophysical property variation in tube flow conducted by Deissler [51] and Oskay and Kakac [52], who studied the variation of viscosity with temperature in a tube in macroscale flow. The concept seems to be well-understood for the macroscale heat transfer problem, but how it affects microscale heat transfer is an ongoing research area. Experimental and numerical studies point out to the non-negligible effects of the variation of especially viscosity with temperature. For example, Nusselt numbers may differ up to 30% as a result of thermophysical property variation in microchannels [53]. Variable property effects have been analyzed with the traditional no-slip/no-temperature jump boundary conditions in microchannels for three-dimensional thermally-developing flow [22] and two-dimensional simultaneously developing flow [23, 26], where the effect of viscous dissipation was neglected. Another study includes the viscous dissipation effect and suggests a correlation for the Nusselt number and the variation of properties [24]. In contrast to the abovementioned studies, the slip velocity boundary condition was considered only recently, where variable viscosity and viscous dissipation effects on pressure drop and the friction factor were analyzed in microchannels [25].

Because of the limited number of studies conducted in this area, simultaneously developing, steady-state, single phase gaseous flow and heat transfer in parallel plate microchannels in the slip flow regime (with slip-flow and temperature-jump boundary conditions) is studied numerically by taking into account the effects of rarefaction, viscous dissipation, and viscosity and thermal conductivity variation with temperature. The geometry is similar to the rough channel geometry, but without the roughness elements. Temperature dependent thermal conductivity is approximated by using a third-order polynomial function

$$k(T) = a_0 T^3 + a_1 T^2 + a_2 T + a_3, \quad (18)$$

where a_i are constants. Temperature dependent dynamic viscosity is modeled by using Sutherland's formula

$$\mu(T) = \mu_0 \frac{T_0 + C}{T + C} \left(\frac{T}{T_0} \right)^{3/2}, \quad (19)$$

where μ_0 is the dynamic viscosity evaluated at the reference temperature T_0 (273 K), and C is the Sutherland constant (111 K for air).

Energy and momentum equations are solved in a coupled manner to account for the viscosity variation. Coupled solutions are made for pressure

and velocity for investigating simultaneously developing flow. Variation of specific heat (C_p) and density (ρ) with temperature is not included, since these properties vary in negligible amounts within the studied temperature range (from 20°C, the inlet temperature, to 85°C, the wall temperature).

The results, grouped into two categories as variable property (vp) and constant property (cp) are presented in Figs. 9–12. Both negative (fluid heating along the channel) and positive (fluid cooling along the channel) Brinkman values are analyzed, with $T_{\text{inlet}}/T_{\text{wall}} = 0.75$ for heating and $T_{\text{inlet}}/T_{\text{wall}} = 1.5$ for fluid cooling. Moreover $Kn = 0.0$ and 0.1 , and $Br = 0.001$, 0.01 , and 0.1 are considered [54].

An examination of Figs. 9–12 shows that the variation of Nu for cp and vp cases differ up to a certain distance in the channel and there is no significant difference in the fully developed Nu values. Both for the cooling and heating cases, the difference due to variable properties is non-negligible for part of the channel length. The difference in the cp and vp local Nu values decreases with increasing Br . An increase in Br , the nondimensional number representing viscous dissipation, results in the development of the flow in a shorter distance, and in return, the temperature gradients decrease. Since the temperature gradients directly affect the variation in properties, an increase in viscous dissipation reduces the difference due to variable properties. Moreover, the difference in the cp and vp local Nu values also decreases slightly with increasing Kn , representing the degree of rarefaction in the flow. As Kn increases, the flow is less affected by the wall conditions. As the heat transfer at the wall decreases, temperature gradients are reduced, and the difference due to variable properties decreases, as explained above.

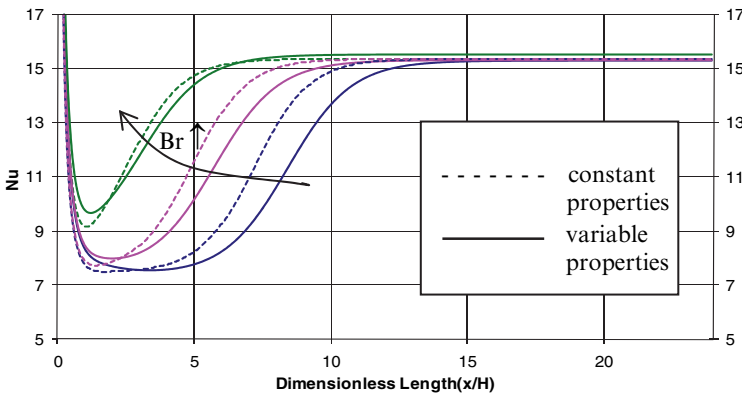


Figure 9. Local Nu variation with positive $Br = 0.001$, 0.01 , 0.1 (fluid cooling) values along the microchannel for $Kn = 0.01$ ($T_{\text{inlet}}/T_{\text{wall}} = 1.5$).

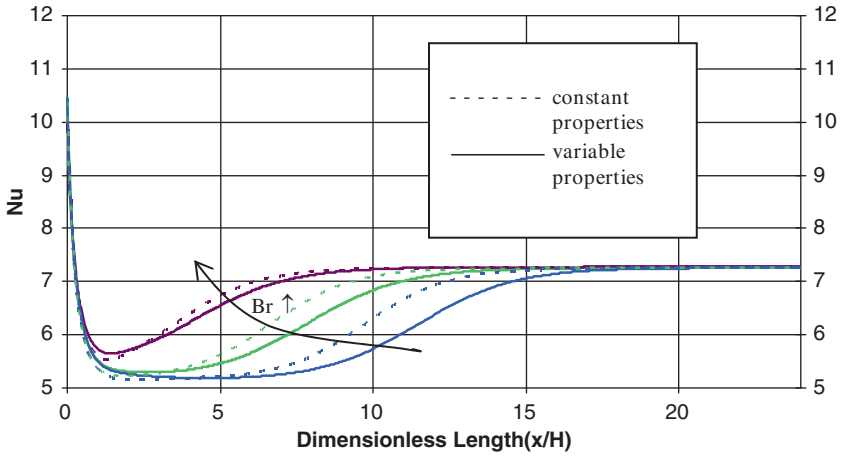


Figure 10. Local Nu variation with positive $Br = 0.001, 0.01, 0.1$ (fluid cooling) values along the microchannel for $Kn = 0.1$ ($T_{inlet}/T_{wall} = 1.5$).

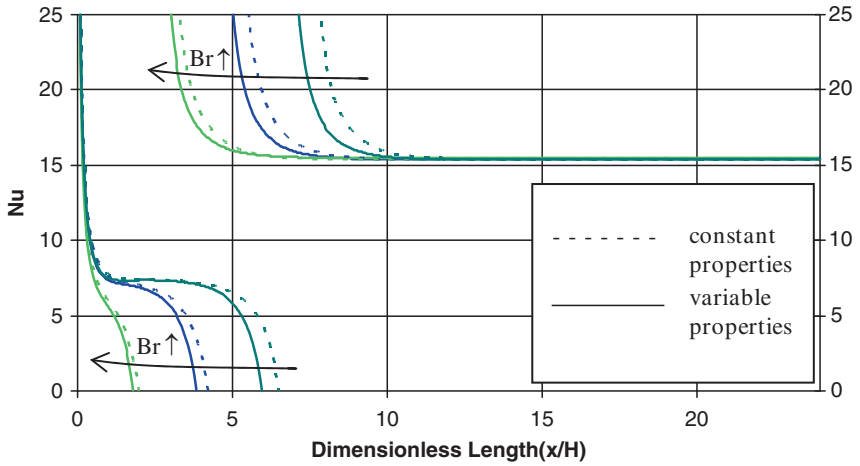


Figure 11. Local Nu variation with negative $Br = -0.001, -0.01, -0.1$ (fluid heating) values along the microchannel for $Kn = 0.01$ ($T_{inlet}/T_{wall} = 0.75$).

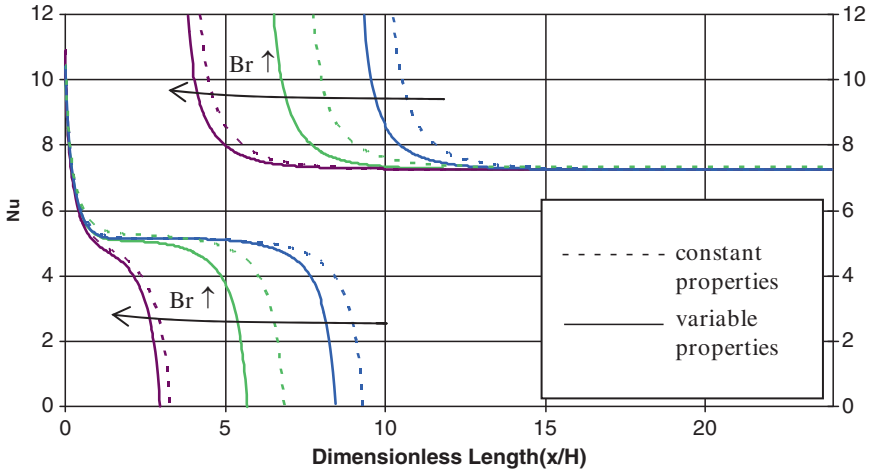


Figure 12. Local Nu variation with negative $Br = -0.001, -0.01, -0.1$ (fluid heating) values along the microchannel for $Kn = 0.1$ ($T_{inlet}/T_{wall} = 0.75$).

6. Conclusions

In this lecture, a variety of results for convective heat transfer in microtubes and microchannels in the slip flow regime under different conditions have been presented. Both constant wall temperature and constant wall heat flux cases have been analyzed in microtubes, including the effects of rarefaction, axial conduction, and viscous dissipation. In rough microchannels the abovementioned effects have also been investigated for the constant wall temperature boundary condition. Then, temperature-variable dynamic viscosity and thermal conductivity of the fluid were considered, and the results were compared with constant property results for microchannels, with the effects of rarefaction and viscous dissipation.

The conclusions drawn for microscale slip flow may be summarized as follows:

1. For high values of rarefaction (high Kn) and temperature jump (high κ), the effect of axial conduction is negligible. However for lower rarefaction and temperature jump values, as Pe decreases (axial conduction effect

- increases), the fully developed Nu increases more significantly. It may be concluded from these observations that the effect of axial conduction should not be neglected for low-rarefied flows and with low values of temperature jump.
2. Regardless of the effect of axial conduction, for a given Kn and κ value, the flow reaches the same fully developed Nu value for all values of Br . When the fluid is cooled ($Br > 0$ for constant wall temperature and $Br < 0$ for constant wall heat flux) Nu takes higher values. The increase in fully developed Nu value with the added effect of viscous dissipation suggests that this effect should not be neglected for long channels. Since micro conduits have high length-to-diameter ratios, even for low values of Br , viscous dissipation effect must be considered.
 3. In general, for constant wall temperature and constant wall heat flux conditions, velocity slip and temperature jump affect the heat transfer in opposite ways: a large slip on the wall will increase the convection along the surface. On the other hand, a large temperature jump will decrease the heat transfer by reducing the temperature gradient at the wall. Therefore, neglecting temperature jump will result in the overestimation of the heat transfer coefficient.
 4. When viscous dissipation is neglected, the effect of axial conduction should be included for $Pe < 100$. When viscous dissipation is included in the analysis, axial conduction is significant for $Pe < 100$ for short channels.
 5. When surface roughness is considered, the fully developed Nu increases with respect to the smooth channel value for rarefied flows, but not for continuum, for all values of Peclet number. The increase in Pe increases Nu more for low values of rarefaction. It appears that, for the range Kn considered in this work, the maximum heat transfer is observed for $Kn = 0.02$. When viscous dissipation effect is included, in either fluid heating or fluid cooling, Nu increases, and more significantly with higher relative roughness values.
 6. The variation of thermophysical properties affects the temperature profile, but not the velocity field. For both fluid heating cooling cases, the variation in local Nu due to temperature-variable properties is significant in the developing region. However the fully developed Nu is almost invariant for constant and variable properties cases due to reduced temperature gradients in this region.

Acknowledgement

The authors would like to thank the Turkish Scientific and Technical Research Council, TUBITAK, Grant No. 106M076, for financial support.

References

1. D.B. Tuckerman and R.F. Pease, Optimized convective cooling using micromachined structure, *Journal of the Electrochemical Society* 129, P. C 98 (1982).
2. P.Y. Wu and W.A. Little, Measurement of heat transfer characteristics of gas flow in fine channels heat exchangers used for microminiature refrigerators, *Cryogenics* 24, 415–420 (1984).
3. S.B. Choi, R.F. Barron, and R.O. Warrington, Fluid flow and heat transfer in microtubes, *Micromechanical Sensors, Actuators, and Systems*, ASME DSC 32, 123–134 (1991).
4. C.P. Tso and S.P. Mahulikar, Experimental verification of the role of Brinkman number in microchannels using local parameters, *International Journal of Heat and Mass Transfer* 43, 1837–1849 (2000).
5. J.Y. Jung and H.Y. Kwak, Fluid flow and heat transfer in microchannels with rectangular cross section, *Heat Mass Transfer* 44, 1041–1049 (2008).
6. H.S. Park and J. Punch, Friction factor and heat transfer in multiple microchannels with uniform flow distribution, *International Journal of Heat and Mass Transfer* 51, 4535–4543 (2008).
7. R.F. Barron, X.M. Wang, R.O. Warrington, and T.A. Ameel, The Graetz problem extended to slip flow, *International Journal of Heat and Mass Transfer* 40, 1817–1823 (1997).
8. T.A. Ameel, R.F. Barron, X.M. Wang, and R.O. Warrington, Laminar forced convection in a circular tube with constant heat flux and slip flow, *Microscale Thermophysical Engineering* 1, 303–320 (1997).
9. B. Cetin, H. Yuncu, and S. Kakac, Gaseous flow in microconduits with viscous dissipation, *International Journal of Transport Phenomena* 8, 297–315 (2006).
10. B. Cetin, A. Guvenc Yazicioglu, and S. Kakac, Fluid flow in microtubes with axial conduction including rarefaction and viscous dissipation, *International Communications in Heat and Mass Transfer* 35, 535–544 (2008).
11. G. Tunc and Y. Bayazitoglu, Heat transfer in microtubes with viscous dissipation, *International Journal of Heat and Mass Transfer* 44, 2395–2403 (2001).
12. G. Tunc and Y. Bayazitoglu, Convection at the entrance of micropipes with sudden wall temperature change, *Proceedings of IMECE*, November 17–22, 2002, New Orleans, Louisiana.
13. S.P. Yu and T.A. Ameel, Slip-flow heat transfer in rectangular microchannels, *International Journal of Heat and Mass Transfer* 44, 4225–4235 (2001).
14. H.-E. Jeong and J.-T. Jeong, Extended Graetz problem including streamwise conduction and viscous dissipation in microchannel, *International Journal of Heat and Mass Transfer* 49, 2151–2157 (2006).
15. Gh.M. Mala and D. Li, Flow characteristics of water in microtubes, *International Journal of Heat and Fluid Flow* 20, 142–148 (1999).
16. C. Kleinstreuer and J. Koo, Computational analysis of wall roughness effect for liquid flow in micro-conduits, *Journal of Fluids Engineering* 126, 1–9 (2004).
17. G. Croce and P. D'Agaro, Numerical analysis of roughness effect on microtube heat transfer, *Superlattices and Microstructures* 35, 601–616 (2004).

18. G. Croce and P. D'Agaro, Numerical simulation of roughness effect on microchannel heat transfer and pressure drop in laminar flow, *Journal of Physics D: Applied Physics* 38, 1518–1530 (2005).
19. G. Croce, P. D'Agaro, and C. Nonini, Three-dimensional roughness effect on microchannel heat transfer and pressure drop, *International Journal of Heat and Mass Transfer* 50, 5249–5259 (2007).
20. G. Croce, P. D'Agaro, and A. Filippo, Compressibility and rarefaction effects on pressure drop in rough microchannels, *Heat Transfer Engineering* 28, 688–695 (2007).
21. Y. Ji, K. Yuan, and J.N. Chung, Numerical simulation of wall roughness on gaseous flow and heat transfer in a microchannel, *International Journal of Heat and Mass Transfer* 49, 1329–1339 (2006).
22. Z. Li, X. Huai, Y. Tao, and H. Chen, Effects of thermal property variations on the liquid flow and heat transfer in microchannel heat sinks, *Applied Thermal Engineering* 27, 2803–2814 (2007).
23. S.P. Guidice, C. Nonino, and S. Savino, Effects of viscous dissipation and temperature dependent viscosity in thermally and simultaneously developing laminar flows in microchannels, *International Journal of Heat and Fluid Flow* 28, 15–27 (2007).
24. J.T. Liu, X.F. Peng, and B.X. Wang, Variable-property effect on liquid flow and heat transfer in microchannels, *Chemical Engineering Journal* 141, 346–353 (2008).
25. M.S. El-Genk and I. Yang, Numerical analysis of laminar flow in micro-tubes with a slip boundary, *Energy Conversion and Management* 50, 1481–1490 (2009).
26. N.P. Gulhane and S.P. Mahulikar, Variations in gas properties in laminar micro-convection with entrance effect, *International Journal of Heat and Mass Transfer* 52, 1980–1990 (2009).
27. M. Gad-El-Hak, The fluid mechanics of microdevices, *Journal of Fluids Engineering* 121, 5–33 (1999).
28. G.L. Morini, Single-phase convective heat transfer in microchannels: A review of experimental results, *International Journal of Thermal Sciences* 43, 631–651 (2004).
29. Y. Bayazitoglu and S. Kakac, Flow regimes in microchannel single-phase gaseous flow, *Microscale Heat Transfer – Fundamentals and Applications in Biological Systems and MEMS*, edited by S. Kakac, L. Vasiliev, Y. Bayazitoglu, and Y. Yener (Kluwer Academic Publishers, The Netherlands 2005).
30. G. Hetsroni, A. Mosyak, E. Pogrebnyak, and L.P. Yarin, Heat transfer in micro-channels: Comparison of experiments with theory and numerical results, *International Journal of Heat and Mass Transfer* 25–26, 5580–5601 (2005).
31. Y. Yener, S. Kakac, M. Avelino, and T. Okutucu, Single phase forced convection in microchannels – State-of art-review, *Microscale Heat Transfer-Fundamentals and Applications in Biological Systems and MEMS*, edited by S. Kakac, L. Vasiliev, Y. Bayazitoglu, and Y. Yener (Kluwer Academic Publishers, The Netherlands 2005).
32. R.M. Cotta, S. Kakaç, M.D. Mikhailov, F.V. Castellós, and C.R. Cardoso, Transient flow and thermal analysis in microfluidics, *Microscale Heat Transfer-Fundamentals and Applications in Biological Systems and MEMS*, edited by

- S. Kakac, L. Vasiliev, Y. Bayazitoglu, and Y. Yener (Kluwer Academic Publishers, The Netherlands 2005).
33. P. Rosa, T.G. Karayiannis, and M.W. Collins, Single-phase heat transfer in microchannels: The importance of scaling, *Applied Thermal Engineering* 29, 3447–3468 (2009).
 34. G. Karniadakis, A. Beskok, and N. Aluru, *Microflows and Nanoflows: Fundamentals and Simulation* (Springer, New York, 2005).
 35. C.B. Sobhan and G.P. Peterson, *Microscale and Nanoscale Heat Transfer: Fundamentals and Engineering Applications* (CRC Press, Florida, 2008).
 36. L.P. Yarin, A. Mosyak, and G. Hetsroni, *Fluid Flow, Heat Transfer and Boiling in Micro-Channels* (Springer, New York, 2008).
 37. Y. Bayazitoglu, G. Tunc, K. Wilson, and I. Tjahjono, Convective heat transfer for single phase gases in microchannel slip flow: Analytical solutions, *Microscale Heat Transfer – Fundamentals and Applications in Biological Systems and MEMS*, edited by S. Kakac, L. Vasiliev, Y. Bayazitoglu, and Y. Yener (Kluwer Academic Publishers, The Netherlands 2005).
 38. N.T. Obot, Toward a better understanding of friction and heat/mass transfer in microchannels – A literature review, *Microscale Thermophysical Engineering* 6, 155–173 (2002).
 39. A. Beskok, G.E. Karniadakis, and W. Trimmer, Rarefaction, compressibility effects in gas microflows, *Journal of Fluids Engineering* 118, 448–456 (1996).
 40. W. Sun, S. Kakac, and A. Guvenc Yazicioglu, A numerical study of single-phase convective heat transfer in microtubes for slip flow, *International Journal of Thermal Sciences* 46, 1084–94 (2007).
 41. B. Cetin, Analysis of single phase convective heat transfer in microtubes and microchannels, M.Sc. Thesis, Middle East Technical University, Ankara, Turkey (2005).
 42. M. Barisik, Analytical solution for single phase microtube heat transfer including axial conduction and viscous dissipation, M.Sc. Thesis, Middle East Technical University, Ankara, Turkey (2008).
 43. G. Tunc and Y. Bayazitoglu, Heat transfer in microtubes with viscous dissipation, *International Journal of Heat and Mass Transfer* 44, 2395–2403 (2001).
 44. S. Kakac and Y. Yener, *Convective Heat Transfer* (CRC Press, Florida, 1994).
 45. R.K. Shah and A.L. London, Laminar flow forced convection in ducts, *Advances in Heat Transfer*, edited by T.F.Jr. Irvine, and J.P. Hartnett (Academic Press, New York 1978), pp. 78–152.
 46. J. Lahjomri and A. Oubarra, Analytical solution of the Graetz problem with axial conduction, *Journal of Heat Transfer* 121, 1078–1083 (1999).
 47. W. Qu, Gh.M. Mala, and D. Li, Heat transfer for water flow in trapezoidal silicon microchannels, *International Journal of Heat and Mass Transfer* 43, 3925–3936 (2000).
 48. J. Koo and C. Kleinstreuer, Analysis of surface roughness effects on heat transfer in micro-conduits, *International Journal of Heat and Mass Transfer* 48, 2625–2634 (2005).
 49. M.B. Turgay and A. Guvenc Yazicioglu, Effect of surface roughness in parallel-plate microchannels on heat transfer, *Numerical Heat Transfer* 56, 497–514 (2009).

50. M.B. Turgay, Effect of surface roughness in microchannels on heat transfer, M.Sc. Thesis, Middle East Technical University, Ankara, Turkey (2008).
51. R.G. Deisler, Analytical investigation of turbulent flow in smooth pipes with heat transfer, with variable fluid properties for Prandtl number of 1, *NACA Technical Note 2242* (1950).
52. R. Oskay and S. Kakac, Effect of viscosity variations on forced convection heat transfer in pipe flow, *METU Journal of Pure and Applied Sciences* 6, 211–230 (1973).
53. H. Herwig and S.P. Mahulikar, Variable property effects in single-phase incompressible flows through microchannels, *International Journal of Thermal Sciences* 45, 977–981 (2006).
54. C. Gozukara, Heat transfer analysis of single phase forced convection in microchannels and microtubes with variable property effect, M.Sc. Thesis, Middle East Technical University, Ankara, Turkey (2010).

Microfluidics Based Microsystems

Fundamentals and Applications

Kakac, S.; Kosoy, B.; Li, D.; Pramuanjaroenkij, A. (Eds.)

2010, X, 618 p., Hardcover

ISBN: 978-90-481-9028-7